Cell Death and Differentiation (2014) 21, 1642–1655

www.nature.com/cdd

A novel PPARγ_2 modulator sLZIP controls the balance between adipogenesis and osteogenesis during mesenchymal stem cell differentiation

J Kim[1] and J Ko*,[1]

Mesenchymal stem cells (MSCs), also known as multipotent stromal cells, are used in clinical trials. However, the use of MSCs for medical treatment of patients poses a potential problem due to the possibility of transdifferentiation into unwanted tissues. Disruption of the balance during MSC differentiation leads to obesity, skeletal fragility, and osteoporosis. Differentiation of MSCs into either adipocytes or osteoblasts is transcriptionally regulated by the two key transcription factors PPARγ_2 and Runx2. PPARγ_2 is highly expressed during adipocyte differentiation and regulates expression of genes involved in adipogenesis. Runx2 induces osteogenic gene expression and, thereby, increases osteoblast differentiation. Although transcriptional modulation of PPARγ_2 has been investigated in adipogenesis, the underlying molecular mechanisms to control the balance between adipogenesis and osteogenesis in MSCs remain unclear. In this study, the role of sLZIP in regulation of PPARγ_2 transcriptional activation was investigated along with sLZIP's involvement in differentiation of MSCs into adipocytes and osteoblasts. sLZIP interacts with PPARγ_2 and functions as a corepressor of PPARγ_2. sLZIP enhances formation of the PPARγ_2 corepressor complex through specific interaction with HDAC3, resulting in suppression of PPARγ_2 transcriptional activity. We found that sLZIP prevents expression of PPARγ_2 target genes and adipocyte differentiation both *in vitro* and *in vivo*. sLZIP also upregulates Runx2 transcriptional activity via inhibition of PPARγ_2 activity, and promotes osteoblast differentiation. sLZIP transgenic mice exhibited enhanced bone mass and density, compared with wild-type mice. These results indicate that sLZIP has a critical role in the regulation of osteogenesis and bone development. However, sLZIP does not affect chondrogenesis and osteoclastogenesis. We propose that sLZIP is a novel PPARγ_2 modulator for control of the balance between adipogenesis and osteogenesis during MSC differentiation, and that sLZIP can be used as a therapeutic target molecule for treatment of obesity, osteodystrophy, and osteoporosis.
Cell Death and Differentiation (2014) **21,** 1642–1655; doi:10.1038/cdd.2014.80; published online 20 June 2014

Mesenchymal stem cells (MSCs) are bone marrow-derived multipotential stromal cells that can differentiate into several distinct cell types, including fat, bone, cartilage, and muscle.[1] Adipogenesis and osteogenesis have a reciprocal relationship in common mesenchymal precursor cells.[2] Disruption of the balance in these processes during MSC differentiation leads to disorders, such as obesity, skeletal fragility, and osteoporosis.[1] MSC differentiation is regulated by specific transcription factors. MSCs differentiate into adipocytes when they express peroxisome proliferator-activated receptor γ_2 (PPARγ_2), which enhances expression of adipogenic genes.[2] Runt-related transcription factor 2 (Runx2) enhances expression of osteogenic genes during osteoblast differentiation; however, PPARγ_2 suppresses osteogenesis via inhibition of Runx2 transcriptional activity.[3] Therefore, characterization of the regulatory mechanism of transcription factors involved in MSC differentiation is important for understanding the developmental processes of adipocytes and osteoblasts.

The nuclear receptor PPARγ is a master regulator in adipogenesis, lipid biosynthesis, inflammation, and glucose metabolism.[2] Binding of PPARγ to specific DNA sequences, including the PPAR response element (PPRE), requires heterodimerization with retinoic X receptor (RXR).[4,5] The heterodimer is associated with the nuclear receptor corepressor complex that includes histone deacetylase (HDAC), nuclear receptor corepressor (NCoR), and the silencing mediator for retinoid and thyroid receptors in the absence of the PPARγ ligand.[6,7] Upon ligand binding, PPARγ undergoes a conformational change and the corepressor complex is replaced by co-activators, including p300, the p160/steroid receptor co-activator (p160/SRC) family, the PPARγ-binding protein, PPARγ co-activator-1 (PGC-1), and the CREB-binding protein.[7,8] Many transcription

[1]Division of Life Sciences, Korea University, Seoul 136-701, Korea
*Corresponding author: J Ko, Division of Life Sciences, Korea University, 5-1 Anam-dong, Seongbuk-gu, Seoul 136-701, Korea. Tel: +822 3290 3445; Fax: +82 2927 9028; E-mail: jesangko@korea.ac.kr
Abbreviations: MSC, mesenchymal stem cells; sLZIP, small leucine zipper protein; PPARγ_2, proliferator-activated receptor γ_2; Runx2, runt-related transcription factor 2; HDAC, histone deacetylases; C/EBP, CCAAT/enhancer-binding protein; AP-1, activator protein 1; FABP4, fatty acid-binding protein 4; LPL, lipoprotein lipase; APL, alkaline phosphatase; OC, osteocalcine; BSP, bone sialoprotein; TZD, thiazolidinediones; Rosi, rosiglitazone; MEF, mouse embryonic fibroblasts; TNT, transcription and translation; TSA, trichostatin A
Received 07.1.14; revised 22.4.14; accepted 09.5.14; Edited by B Zhivotovsky; published online 20.6.14

factors and ligands are involved in expression and function of PPARγ. Transcription factors of the CCAAT/enhancer-binding protein (C/EBP) family stimulate PPARγ transcription by binding directly to the promoter of PPARγ.[9] The natural PPARγ ligand 15-deoxy-Δ12,14-prostaglandin J2, and a synthetic class of thiazolidinediones (TZDs), including troglitazone, pioglitazone, and rosiglitazone, also activate the transcriptional activity of PPARγ.[6] Negative regulators, including TAZ, the retinoblastoma protein (pRb), and cyclin D1, inhibit PPARγ transcriptional activity, and CREB suppresses hepatic PPARγ expression in a fasted state.[10–12] The leucine zipper protein (LZIP) is a member of a large family of bZIP transcription factors.[13] The N-terminal 92 amino-acid region of LZIP contains a potent transactivation domain that consists of two LxxLL nuclear receptor interaction motifs.[14] Recently, a novel isoform of human LZIP, known as small LZIP (sLZIP), has been identified.[15] sLZIP consists of 354 amino acids and lacks the putative transmembrane domain of LZIP.[15] sLZIP decreases the LxxLL motif-dependent transcriptional activity of the glucocorticoid receptor (GR) by recruiting and activating HDACs.[15] In this study, we investigated the roles of sLZIP in regulation of the transcriptional activities of PPARγ_2 and Runx2, and in osteogenesis and adipogenesis. We propose a novel mechanism whereby sLZIP is a key regulator in controlling the balance between adipogenesis and osteogenesis during MSC differentiation.

Results

sLZIP inhibits adipogenesis via suppression of PPARγ_2 transcriptional activity. As sLZIP contains two LxxLL motifs that are essential for interaction with nuclear receptors,[15] the role of sLZIP in regulation of PPARγ_2 transactivation during MSC differentiation was investigated. To examine the effect of sLZIP on the transcriptional activity of PPARγ_2, sLZIP, and the PPRE-containing FABP4 promoter reporter gene (FABP4-Luc) were transfected into 293T cells. The transcriptional activity of PPARγ_2 was increased 4.2-fold in response to ligands; however, sLZIP inhibited PPARγ_2 transactivation. (Figure 1a and Supplementary Figures S1a and b). LZIP also decreased the transcriptional activity of PPARγ_2 by 32%; however, the effect of LZIP on PPARγ_2 transactivation was less than the effect of sLZIP (Supplementary Figures S1c and d). Suppression of sLZIP expression using siRNA against sLZIP (si-sLZIP) enhanced PPARγ_2 transcriptional activity in a dose-dependent manner (Figure 1b). To investigate whether endogenous PPARγ_2 transcriptional activity is regulated by sLZIP, C3H10T1/2 mesenchymal cells stably expressing the FABP4 reporter gene were infected with the sLZIP-expressing adenovirus, followed by differentiation into adipocytes. sLZIP decreased the transcriptional activity of PPARγ_2 by $\sim$60% (Figure 1c), and inhibited FABP4 expression in a dose-dependent manner in adipocytes (Supplementary Figure S1e). We investigated whether sLZIP is involved in heterodimer formation of PPARγ_2 with RXR. PPARγ_2 transcriptional activity was increased by 13-fold in response to rosiglitazone, compared with a control; however, sLZIP decreased the transcriptional activity of the PPARγ_2/RXR heterodimer in a dose-dependent manner (Figure 1d). The negative effect of sLZIP on PPARγ_2 transcriptional activity was abrogated in an RXR-dose-dependent manner when cells were expressed with increasing amounts of RXR (Figure 1e). Results of a GST pull-down assay showed that sLZIP interacts with the PPARγ_2/RXR heterodimer; however, sLZIP did not affect heterodimer formation (Supplementary Figure S1f). To investigate the effect of sLZIP on adipogenesis, sLZIP transgenic (TG) mice were generated (Supplementary Figure S2), and pre-adipocyte cells were isolated from an epididymal fat pad of sLZIP TG mice. PPARγ_2 transcriptional activity was decreased by 21% in adipocytes of sLZIP TG mice, compared with wild-type (WT) mice (Figure 1f). Mouse LZIP slightly decreased the transcriptional activity of PPARγ_2, compared with a control (Supplementary Figure S3a). Endogenous expressions of both human sLZIP and the homologous gene of sLZIP in mice (mLZIP) were decreased during the process of differentiation (Supplementary Figures S3b–d). We next examined the effect of sLZIP on adipocyte differentiation using multipotent mesenchymal and pre-adipocyte cells. C3H10T1/2 and 3T3-L1 cells were infected with an adenovirus expressing sLZIP, and allowed to differentiate into adipocytes. sLZIP apparently inhibits differentiation of C3H10T1/2 and 3T3-L1 cells into adipocytes (Figure 1g and Supplementary Figure S3e). Knockdown of sLZIP increased differentiation of human MSCs into adipocytes (Supplementary Figure S3f). We examined the effect of sLZIP on adipocyte differentiation *in vivo*. Differentiation of primary pre-adipocytes and mouse embryonic fibroblasts (MEFs) isolated from sLZIP TG mice was inhibited, compared with WT mice (Figures 1h and i). The same effects were observed in pre-adipocytes of LZIP TG mice (Supplementary Figures S3g and h). In addition, the fat mass of sLZIP TG mice was significantly reduced by 38%, compared with WT mice (Figure 1j). Expressions of *FABP4* and other PPARγ_2 target genes, including *C/EBPα* and *LPL*, were downregulated in sLZIP TG mice by 68%, 42%, and 76%, respectively, compared with WT mice (Figure 1k). These results indicate that sLZIP functions as a negative regulator in adipogenic differentiation both *in vitro* and *in vivo* via suppression of PPARγ_2 transcriptional activity.

sLZIP interacts with PPARγ_2. To investigate whether the transcriptional activity of PPARγ_2 is affected by the interaction of PPARγ_2 with sLZIP, we examined the interaction between sLZIP and PPARγ_2. Results from a GST pull-down assay showed that sLZIP interacts with PPARγ_2 (Figure 2a). Results from a His pull-down assay using purified His-sLZIP and *in vitro* translated PPARγ_2 showed that PPARγ_2 binds directly to sLZIP (Figure 2b). In addition, sLZIP is colocalized with PPARγ_2 in the nucleus (Figure 2c). To investigate whether the LxxLL motifs of sLZIP are important for the interaction with PPARγ_2, we generated two LxxLL mutant constructs of sLZIP (Supplementary Figure S4a). The WT and the second sLZIP mutant (^{54}LxxAA) interacted with PPARγ_2; however, the first sLZIP mutant (^{13}LxxAA) and the double sLZIP mutant weakly interacted with PPARγ_2 (Supplementary Figure S4b). sLZIP mutants did not affect

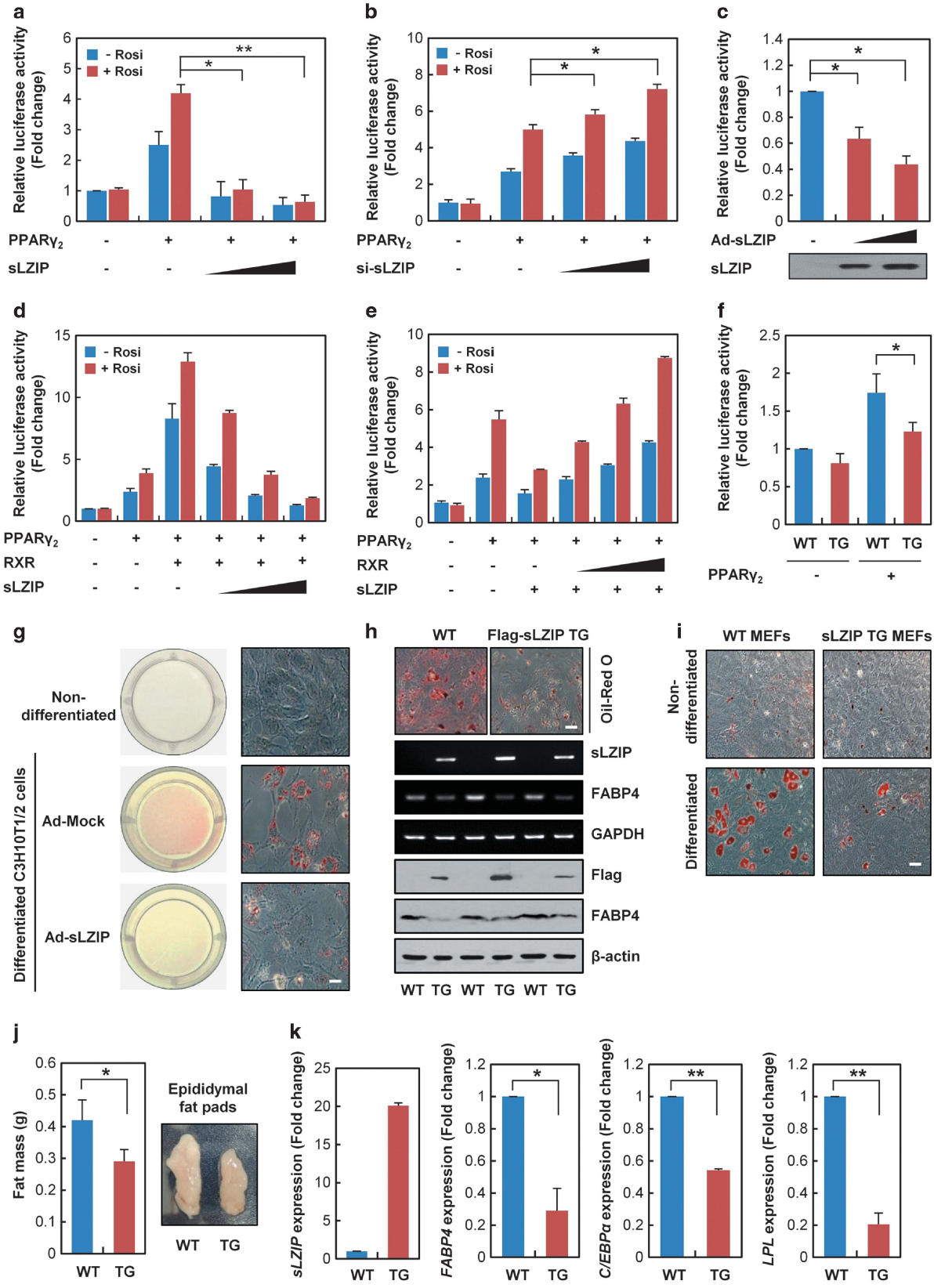
a
Relative luciferase activity (Fold change)
- Rosi
+ Rosi
PPARγ2
sLZIP
b
Relative luciferase activity (Fold change)
- Rosi
+ Rosi
PPARγ2
si-sLZIP
c
Relative luciferase activity (Fold change)
Ad-sLZIP
sLZIP
d
Relative luciferase activity (Fold change)
- Rosi
+ Rosi
PPARγ2
RXR
sLZIP
e
Relative luciferase activity (Fold change)
- Rosi
+ Rosi
PPARγ2
RXR
sLZIP
f
Relative luciferase activity (Fold change)
WT TG WT TG
PPARγ2
g
Non-differentiated
Differentiated C3H10T1/2 cells
Ad-Mock
Ad-sLZIP
h
WT
Flag-sLZIP TG
Oil-Red O
sLZIP
FABP4
GAPDH
Flag
FABP4
β-actin
WT TG WT TG WT TG
i
WT MEFs
sLZIP TG MEFs
Non-differentiated
Differentiated
j
Fat mass (g)
WT TG
Epididymal fat pads
WT TG
k
sLZIP expression (Fold change)
FABP4 expression (Fold change)
C/EBPα expression (Fold change)
LPL expression (Fold change)
WT TG

PPARγ_2 transcriptional activity, indicating that the LxxLL motifs of sLZIP are not involved in regulation of PPARγ_2 transcriptional activity (Supplementary Figure S4c). We next investigated which domain of sLZIP is required for binding to PPARγ_2. Various sLZIP deletion mutants, including sLZIP N (1-228), sLZIP C (229–354), and sLZIP CC (297–354), were constructed, and the PPARγ_2-binding domain was analyzed using a GST pull-down assay. sLZIP WT, sLZIP C, and sLZIP CC all interacted with PPARγ_2, whereas sLZIP N did not bind to PPARγ_2 (Figure 2d). These results indicate that sLZIP CC (297–354) containing the proline-rich region is important for binding to PPARγ_2. The domain of PPARγ_2 that is required for binding to sLZIP was also identified. The ligand-binding domain (AF-2) of PPARγ_2 is necessary for binding to sLZIP (Figure 2e). These results suggest that sLZIP CC (297–354) interacts with the AF-2 domain of PPARγ_2.

HDAC3 is involved in sLZIP suppression of PPARγ_2 transcriptional activity. To investigate the sLZIP regulatory mechanism of PPARγ_2 transcriptional activity, we examined whether HDACs are involved in sLZIP-mediated repression of PPARγ_2 transactivation. In the absence of the HDAC inhibitor trichostatin A (TSA), sLZIP inhibited PPARγ_2 transcriptional activity; however, sLZIP did not affect PPARγ_2 transcriptional activity in cells treated with TSA (Figure 3a), indicating that HDACs are involved in sLZIP-mediated repression of PPARγ_2 transactivation. The HDAC isoform that is involved in this event was investigated. Results of an immunoprecipitation assay showed that sLZIP specifically interacts with HDAC3 (Figure 3b). Results of a GST pull-down assay confirmed the interaction between sLZIP and HDAC3 (Figure 3c). In addition, sLZIP is colocalized with HDAC3 in the nucleus (Figure 3d). We examined whether interaction of sLZIP with HDAC3 is required for repression of PPARγ_2 transcriptional activity. As shown in Figure 3e, siRNAs against HDAC1, 2, and 8 did not affect sLZIP-mediated PPARγ_2 regulation. However, knockdown of HDAC3 abrogated PPARγ_2 transcriptional activity that was suppressed by sLZIP (Figure 3e). Co-transfection with both sLZIP and HDAC3 completely inhibited PPARγ_2 transcriptional activity in both the presence and absence of rosiglitazone (Figure 3f). We also investigated the interaction between sLZIP and the corepressor complex of PPARγ_2 in the presence of the PPARγ_2 ligand. sLZIP interacted with HDCA3 in both the presence and absence of rosiglitazone (Figure 3g). However, the interaction between sLZIP and NCoR1 was weak in the presence of the PPARγ_2 ligand (Figure 3h). These results indicate that sLZIP negatively regulates PPARγ_2 transcriptional activity via recruitment of HDAC3 to the corepressor complex of PPARγ_2.

sLZIP enhances formation of the PPARγ_2 corepressor complex. We investigated whether sLZIP binds to PPARγ_2 in response to ligands. sLZIP interacted with PPARγ_2 in the absence of rosiglitazone; however, sLZIP did not bind to PPARγ_2 in the presence of rosiglitazone (Figure 4a). To confirm the ligand-dependent dissociation of sLZIP from PPARγ_2, we examined the time dependency of the interaction between sLZIP and PPARγ_2. As shown in Figure 4b, sLZIP dissociated from PPARγ_2 in a time-dependent manner. We examined whether the ligand-dependent interaction between sLZIP and PPARγ_2 is involved in the regulation of PPARγ_2 transcriptional activity. sLZIP inhibited PPARγ_2 transcriptional activity in both the presence and absence of rosiglitazone (Figure 4c). In addition, PPARγ_2 transcriptional activity was slightly inhibited by the sLZIP (1–220) deletion mutant, which lacks the PPARγ_2-binding site (Figure 4c). As sLZIP (1–220) contains the DNA-binding domain and is involved in interaction with HDAC3, sLZIP probably regulates PPARγ2 transactivation via binding together with HDAC3 to the promoter region of PPARγ_2 target genes. We investigated the effect of sLZIP on interaction between PPARγ_2 and HDAC3. HDAC3 dissociates from PPARγ_2 after treatment with rosiglitazone; however, sLZIP enhanced the interaction between PPARγ_2 and HDAC3 (Figure 4d). We next investigated whether sLZIP is involved in ubiquitination of HDAC3. Rosiglitazone increased ubiquitination of HDAC3; however, sLZIP blocked ubiquitination-dependent degradation of HDAC3 (Figure 4e). sLZIP also inhibited recruitment of the co-activator PGC-1α to PPARγ_2 (Figure 4f). These results suggest that sLZIP regulates PPARγ_2 transcriptional activity by interacting with PPARγ_2, and inhibits corepressor degradation by enhancing formation of the corepressor complex.

sLZIP binds to the enhancer region of FABP4. During adipogenesis, PPARγ_2 binds to the enhancer of the FABP4 gene ($\sim$5 kb), which contains the two PPARγ_2-binding

Figure 1 sLZIP inhibits adipogenesis via suppression of PPARγ_2 transcriptional activity. (**a**) 293T cells were transfected with PPARγ_2, β-galactosidase, FABP4-Luc, and various amounts of sLZIP (0.25 and 0.5 μg), and stimulated with or without 10 μM of rosiglitazone (Rosi) for 24 h. Promoter activity was determined using a luciferase assay. *$P<0.01$, **$P<0.005$. (**b**) 293T cells were transfected with various amounts of si-sLZIP (50 and 100 nM), and treated with or without 10 μM Rosi for 24 h. *$P<0.01$. (**c**) C3H10T1/2 cells stably expressing the FABP4 reporter gene were infected with sLZIP-expressing adenovirus, followed by differentiation into adipocytes for 4 days. *$P<0.05$. (**d**, **e**) 293T cells were transfected with PPARγ_2, β-galactosidase, FABP4-Luc, and various amounts of sLZIP (0.1, 0.25, and 0.5 μg) and RXR (0.1, 0.25, and 0.5 μg). Following transfection, cells were stimulated with or without 10 μM Rosi for 24 h. Luciferase activity was normalized to β-galactosidase activity and presented as the relative activity. (**f**) Pre-adipocyte cells were isolated from epididymal fat pads of WT and sLZIP TG mice. Cells were then transfected with FABP4-Luc and PPARγ_2, and treated with or without 10 μM Rosi for 24 h. Promoter activity was measured by a luciferase assay. *$P<0.01$. (**g**) C3H10T1/2 cells were infected with sLZIP-expressing adenovirus and differentiated into adipocytes. After 8 days from post-induction, cells were stained with Oil Red O. Scale bar, 50 μm. (**h**) Pre-adipocyte cells were isolated from epididymal fat pads of WT and sLZIP TG mice, and differentiated into adipocytes. After 8 days from post-induction, cells were stained with Oil Red O, and the expression level of FABP4 was determined using RT-PCR and Western blot analysis. Scale bar, 50 μm. (**i**) MEF cells isolated from WT and sLZIP TG mice were differentiated into adipocytes. Cells were stained with Oil Red O. Scale bar, 50 μm. (**j**) The white adipose tissue (fat) mass of WT and sLZIP TG mice. *$P<0.05$. (**k**) Total RNA was extracted and the mRNA level of PPARγ_2 target genes (*FABP4, C.EBP1,* and *LPL*) were determined using real-time PCR after 8 days from post-induction. GAPDH was used as an internal control. *$P<0.005$, **$P<0.001$. All experiments were performed in triplicate and the bar represents the mean $\pm$ S.D.

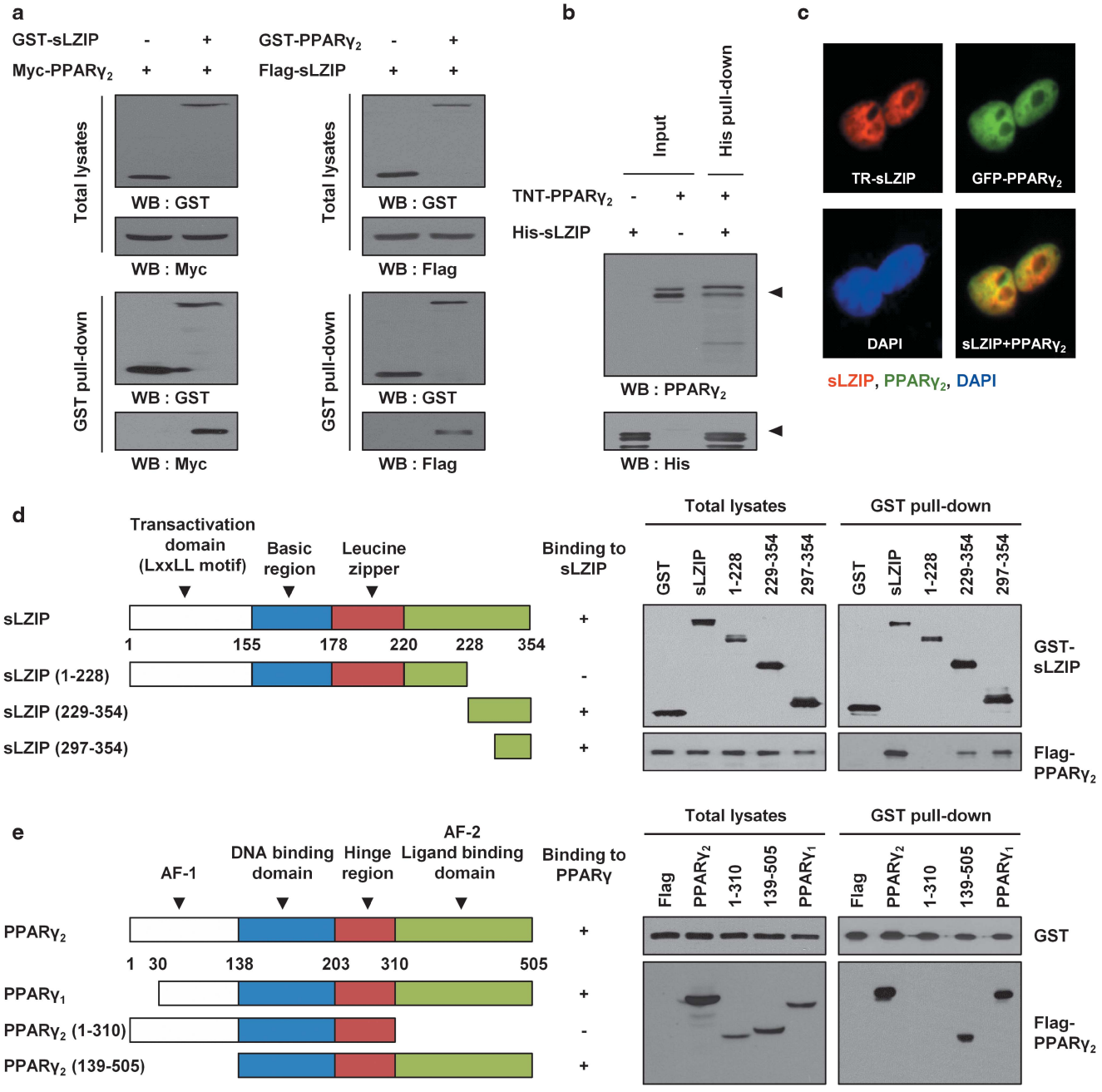

Figure 2 sLZIP interacts with PPARγ_2. (**a**) GST-sLZIP, Myc-PPARγ_2, GST-PPARγ_2, and Flag-sLZIP were co-transfected into 293T cells. Cell lysates were collected and GST pull-down assays were performed using glutathione 4B beads. (**b**) PPARγ_2 was *in vitro* translated using a TNT translation reaction, and His-sLZIP proteins were expressed in BL21 cells. Purified His-sLZIP proteins were subjected to a His pull-down assay. (**c**) GFP-PPARγ_2 and Flag-sLZIP constructs were expressed into C3H10T1/2 cells and analyzed by fluorescence microscopy using Texas Red-conjugated anti-Flag antibody. The nucleus was stained with DAPI. (**d**) 293T cells were transfected with GST-sLZIP (1-354), GST-sLZIP (1-228), GST-sLZIP (229–354), GST-sLZIP (297–354), and Flag-PPARγ_2. (**e**) 293T cells were transfected with Flag-PPARγ_2 (1-505), Flag-PPARγ_2 (1-310), Flag-PPARγ_2 (139-505), Flag-PPARγ_1, and GST-sLZIP. GST pull-down assays were performed using glutathione 4B beads. Protein complex was analyzed on SDS-PAGE, followed by western blotting using anti-GST and anti-Flag antibodies

elements of ARE6 and ARE7.[5] PPARγ_2 does not bind to the PPARγ_2-binding element in the proximal region (~2 kb) of the FABP4 gene during adipogenesis.[16] The putative sLZIP-binding sites in the FABP4 enhancer region were identified (Figure 5a). We investigated the DNA-binding ability of sLZIP to these elements in the FABP4 enhancer. sLZIP bound directly to the CREB-binding site near ARE6 and ARE7; however, sLZIP did not bind to the C/EBP and AP-1 sites (Figure 5b). The DNA-binding ability of sLZIP was increased in a dose-dependent manner (Figure 5c). However, sLZIP did not bind to the CREB-binding site in the presence of the cold competitor, and treatment with the

His antibody induced a supershift (Figure 5c). sLZIP did not bind to the CREB-binding site mutant (TG*AT*GTCA→TG*GG*GTCA) (Figure 5d). A chromatin immunoprecipitation assay (ChIP) was also performed. sLZIP was recruited to the CREB-binding site of the FABP4 enhancer in both the presence and absence of rosiglitazone (Figure 5e). To further investigate the DNA-binding ability of sLZIP to the FABP4 enhancer, the transcriptional activity of PPARγ_2 was investigated using FABP4 enhancer-luciferase constructs. sLZIP decreased the transcriptional activity of PPARγ_2 in a dose-dependent manner (Figure 5f). These results indicate that sLZIP binds to the CREB-binding site of the FABP4 enhancer, and leads to formation of the PPARγ_2 corepressor complex.

sLZIP promotes osteogenesis via enhancement of Runx2 transcriptional activity. We investigated the role of sLZIP in the regulation of Runx2 transcriptional activity. sLZIP increased the transcriptional activity of Runx2 by 4.2-fold, whereas si-sLZIP decreased Runx2 transcriptional activity in a dose-dependent manner (Figures 6a and b). PPARγ_2 inhibited the transcriptional activity of Runx2 by ~50%; however, sLZIP abrogated the transcriptional activity of Runx2 that was repressed by PPARγ_2 (Figure 6c). We examined whether HDAC3 is involved in sLZIP-mediated regulation of Runx2 transcriptional activity. HDAC3 decreased Runx2 transcriptional activity; however, sLZIP recovered the transcriptional activity of Runx2 in a dose-dependent manner (Figure 6d). The effect of sLZIP on differentiation of MSCs to osteoblasts was investigated. sLZIP increased the differentiation of primary human MSCs and C3H10T1/2 cells into osteoblasts; however, knockdown of sLZIP decreased osteoblast differentiation (Figure 6e). We also examined osteoblast differentiation in MEFs isolated from sLZIP TG mice. sLZIP promotes both osteoblast differentiation and bone nodule formation (Figure 6f and Supplementary Figure S5). Furthermore, sLZIP upregulated expressions of the Runx2 target genes, including alkaline phosphatase, osteocalcin (*OC*), and bone sialoprotein by 4.2-, 2.9- and 3.4-fold, respectively (Figure 6g). These results suggest that sLZIP enhances the transcriptional activity of Runx2 via inhibition of PPARγ_2 activity and, thereby, induces osteoblast differentiation.

sLZIP enhances bone mass *in vivo*. To investigate the physiological role of sLZIP during the process of bone formation, we performed a histological analysis using the distal femur and the proximal tibia isolated from sLZIP TG mice. Results showed a thickened cortical bone and increased mass trabecular bones in the femur, compared with WT mice (Figure 7a and Supplementary Figure S6a). Bone histomorphometric analysis confirmed the observed increase in the bone volume (BV) of sLZIP TG mice. The bone mineral density and the BV/tissue volume of sLZIP TG mice were significantly increased by 25% and 36%, respectively, compared with WT mice (Figure 7b). To investigate detailed static bone histomorphometry, the thickness (Tb. Th.), bone number (Tb. N.), and separation (Tb. Sp.) of trabeculae were all measured in WT and sLZIP TG mice. The bone number and the thickness of the trabeculae were increased by 31% and 22%, respectively and the trabecular bone separation was decreased by 29% in sLZIP TG mice, compared with WT mice (Figure 7b). Similar results were observed using two- and three-dimensional micro-CT analyses of the distal part of the femur and the proximal part of the tibia (Figures 7c–e). The effect of sLZIP on ossification (or osteogenesis) *in vivo* was evaluated. Staining with cartilage-specific Alcian Blue and bone-specific Alizarin Red at E17.5 revealed that the skulls and limbs of sLZIP TG mouse embryos exhibited accelerated ossification, compared with WT mice (Figure 7f). In addition, results of whole skeletal staining showed that the skulls of sLZIP TG mice were slightly larger than the skulls of WT mice (Figure 7f). A bone, when first starting to develop during embryogenesis, is formed of cartilage that is subsequently replaced bone in a process called ossification.[17] To investigate whether sLZIP-mediated bone formation is involved in cartilage development, we examined the effect of sLZIP on chondrocyte differentiation. ATDC5 chondrogenic cells were treated with insulin and allowed to differentiate into chondrocytes. In the presence of insulin, sLZIP did not affect expression of the chondrocyte differentiation marker genes, including *Sox9* and *ColIIIA1* (Supplementary Figure S6b). Staining with Alcian Blue at E12.5 revealed that the limbs and tails of sLZIP TG mouse embryos exhibited no difference from WT embryos (Supplementary Figure S6c). Bone homeostasis is maintained by a balance between bone formation by osteoblasts and bone resorption by osteoclasts in vertebrates.[18] Osteoblasts not only have a role in bone formation, but also regulate osteoclastogenesis.[19] To investigate whether sLZIP regulates osteoclast differentiation, bone marrow macrophages isolated from sLZIP TG mice were differentiated into osteoclasts. There were no differences between WT and sLZIP TG mice in expression of the osteoclast markers *Oscar, CTSK*, and *TRAP* (Supplementary Figure S6d). These findings point to a novel mechanism whereby sLZIP represses adipogenesis and promotes osteogenesis via modulation of the transcriptional activities of PPARγ_2 and Runx2 in MSCs.

Discussion

sLZIP decreases the transcriptional activity of GR by recruiting and activating HDACs.[15] PPARγ_2 contains a C-terminal ligand-binding domain that has an activation domain (AF2).[20] The LxxLL motif, which is found in most co-regulators, is important for interaction between the nuclear receptor and the co-regulator via AF2.[20] sLZIP has two LxxLL motifs in the transactivation domain that are critical for modulation of GR activity.[15] Therefore, the present study investigated the relationship between sLZIP and PPARγ transcriptional activation. sLZIP inhibits PPARγ_2 transcriptional activity via interaction with PPARγ_2; however, the LxxLL motifs of sLZIP were not necessary for regulation of PPARγ_2 transactivation. sLZIP dissociates from PPARγ_2 after treatment with the PPARγ_2 ligand, as do other PPARγ_2 corepressors. However, the inhibitory effect of sLZIP on PPARγ_2

transcriptional activity is retained. sLZIP (1–220), containing the DNA-binding domain and the HDAC3 interaction domain, inhibited PPARγ_2 transcriptional activity although it lacks the PPARγ_2 interaction domain. Our results indicate that sLZIP binds to the CREB-binding site of the FABP4 enhancer, leading to the inhibition of HDAC3 degradation by enhancing

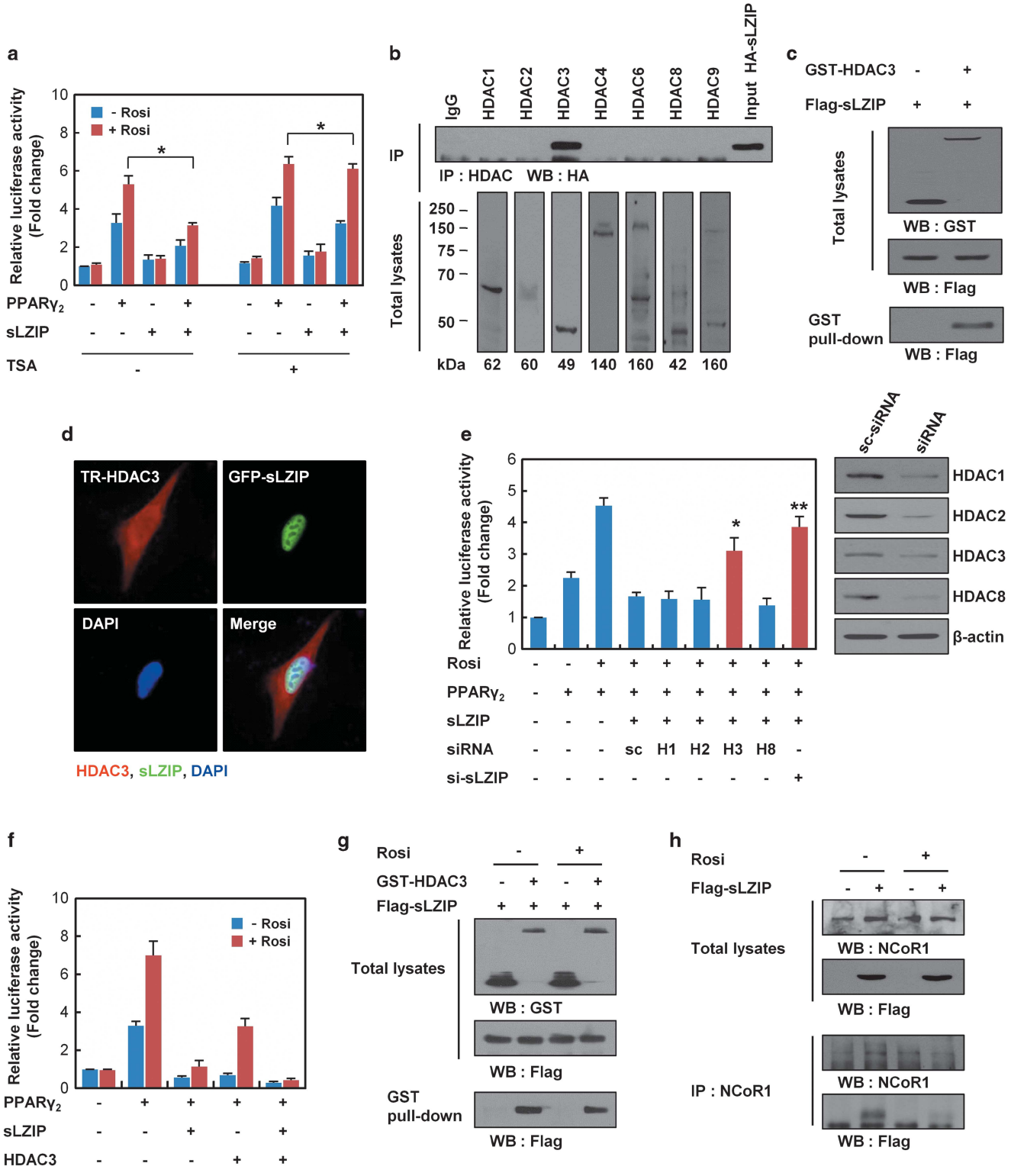

the formation of the corepressor complex (Supplementary Figure S7a and b). Two homologous mouse LZIPs have been identified and designated as mouse LZIP-1 and LZIP-2.[21] Mouse LZIP also decreases the transcriptional activity of PPARγ_2; however, the effect is much less than for human sLZIP. Therefore, we generated human sLZIP TG mice and the role of sLZIP in adipogenesis was investigated. Consistent with *in vitro* results, adipocyte differentiation was inhibited in both primary pre-adipocytes and MEFs isolated from sLZIP TG mice.

Adipocyte and osteoblast differentiation of MSCs is reversely regulated by critical differentiation regulators. The transcriptional co-activator with PDZ-binding motif (TAZ) stimulates transcription of the Runx2-dependent gene OC, a late marker of osteoblast development, and represses PPARγ_2-dependent gene transcription via interaction with PPARγ_2.[12] Adipocyte differentiation is enhanced in MEFs isolated from TAZ knockout mice, whereas bone formation is inhibited in TAZ-depleted zebra fish embryos.[12] Vascular endothelial growth factor (VEGF) also regulates the balance between adipocyte and osteoblast differentiation. A VEGF deficiency in osteoblastic precursor cells causes development of an osteoporosis-like phenotype and increased bone marrow fat.[22] The homeobox protein MSX-2 (Msx2) inhibits both the expression and transcriptional activity of PPARγ , and blocks adipocyte differentiation of MSCs; however, Msx2-deficient mice show defects in skull ossification and decreased numbers of osteoblasts.[23]

Osteogenesis is regulated by many of the major developmental signaling pathways, including the bone morphogenetic protein (BMP), Wnt, and Runx2 pathways.[17] Runx2 is expressed at the site of bone formation and is a key transcription factor of osteoblast differentiation.[3] Activation of PPARγ_2 inhibits Runx2-mediated transcription, whereas PPARγ_2-deficient mice show increased bone mass via stimulation of osteoblastogenesis.[24] Clinical surveys indicate that the long-term use of the drug TZDs by diabetes patients leads to an increase in the fat ratio and to bone loss, and MSCs from osteoporosis patients are more differentiated into adipocytes than osteoblasts, compared with patients with normal bone mass.[25] sLZIP enhances osteoblast differentiation and bone development via upregulation of the transcriptional activity of Runx2 and downregulation of PPARγ_2 transactivation (Supplementary Figure S7c). A recent study has reported that the LZIP homolog gene OASIS is induced by BMP2 signaling in osteoblasts and results in increased bone formation.[26] In addition, glucocorticoids suppress bone formation by attenuating osteoblastogenesis via interaction of monomeric GR with AP-1.[19] sLZIP functions as a negative regulator in glucocorticoid-induced transcriptional activation of GR.[15] Therefore, sLZIP probably has a critical role in controlling the balance of adipocyte and osteoblast differentiation via regulation of the activities of nuclear receptors.

Although numerous studies have described MSC differentiation, the molecular mechanism to control the balance between adipogenesis and osteogenesis in MSCs remains unclear. The present study showed that sLZIP inhibits the transcriptional activity of PPARγ_2 in both the presence and absence of a ligand via interaction with the corepressor complex, including HDAC3. sLZIP binds directly to the CREB-binding site of the FABP4 enhancer, leading to the enhancement of PPARγ_2 corepressor complex formation. sLZIP inhibits adipogenic differentiation both *in vitro* and *in vivo*. sLZIP increases the transcriptional activity of Runx2 via suppression of PPARγ_2 transcriptional activity and promotes osteoblast differentiation in both MSCs and MEF cells of sLZIP TG mice, leading to bone mass enhancement.

This is the first report of a novel mechanism whereby sLZIP functions as a key regulator to control the balance between adipogenesis and osteogenesis. Therefore, sLZIP is a potentially useful therapeutic target molecule for a medical approach to treatment of skeletal dysplasia, osteoporosis, hypertrophic obesity, and the metabolic syndrome.

Materials and Methods

Materials. Dulbecco's modified Eagle's medium (DMEM), RPMI 1640, penicillin, and streptomycin were purchased from Invitrogen (Carlsbad, CA, USA). Fetal bovine serum (FBS) was purchased from Hyclone Laboratory (Cat. no. SH30919.03). Antibodies against PPARγ_2, HDACs (1, 2, 3, 4, 6, 8, and 9), RXRα, NCoR1, PGC1α, and β-actin were obtained from Santa Cruz Biotechnology (Santa Cruz, CA, USA). Anti-mouse and anti-rabbit peroxidase-conjugated secondary antibodies were purchased from Pierce (Madison, WI, USA). Insulin, methylisobutylxanthine (IBMX), β-glycerophosphate, ascorbic acid, dexamethasone, Alizarin Red, Oil Red O, troglitazone, and pioglitazone were purchased from Sigma-Aldrich (St Louis, MO, USA). Rosiglitazone was purchased from Enzo Life Science (Farmingdale, NY, USA).

Cell culture and differentiation. Primary human MSCs were purchased from Lonza (Walkersville, MD, USA) and grown in DMEM supplemented with 10% FBS and penicillin (100 U/ml)/streptomycin (100 μg/ml). MEF cells were isolated from 12.5-day-old-WT and sLZIP TG mouse

Figure 3 HDAC3 is involved in sLZIP suppression of PPARγ_2 transcriptional activity. (**a**) 293T cells were transfected with FABP4-Luc, β-galactosidase, PPARγ_2, and sLZIP. Following transfection, cells were stimulated with or without 10 μM Rosi and 100 nM TSA. Promoter activity was determined by a luciferase assay. *$P<0.005$. (**b**) HA-sLZIP was transfected into 293T cells. Cell lysates were collected and immunoprecipitation assays were performed using the indicated antibodies. (**c**) GST-HDAC3 and Flag-sLZIP were co-transfected into 293T cells. Cell lysates were collected and GST pull-down assays were performed using glutathione 4B beads. (**d**) GFP-sLZIP were expressed into C3H10T1/2 cells and analyzed by fluorescence microscopy using Texas Red-conjugated anti-HDAC3 antibody. The nucleus was stained with DAPI. (**e**) 293T cells were transfected with FABP4-Luc, β-galactosidase, PPARγ_2, sLZIP, and 100 nM siRNAs against scramble (sc), sLZIP, HDAC1, 2, 3, and 8 (H1, H2, H3, and H8, respectively). After transfection, cells were stimulated with or without 10 μM Rosi for 24 h, and promoter activity was determined. *$P<0.01$; **$P<0.005$. (**f**) 293T cells were co-transfected with FABP4-Luc, β-galactosidase, PPARγ_2, HDAC3, and sLZIP. Following transfection, cells were stimulated with or without 10 μM Rosi for 24 h and subjected to a luciferase assay. Luciferase activities were normalized to the β-galactosidase activity and presented as the relative activity. (**g**) 293T cells were transfected with GST-HDAC3 and Flag-sLZIP, and treated with or without 10 μM Rosi for 24 h. Cell lysates were subjected to a GST pull-down assay. (**h**) Flag-sLZIP was expressed into 293T cells. Cells were treated with 10 μM Rosi for 24 h. Cell extracts were analyzed by an immunoprecipitation assay using an anti-NCoR1 antibody. Protein complex was analyzed on SDS-PAGE, followed by western blotting

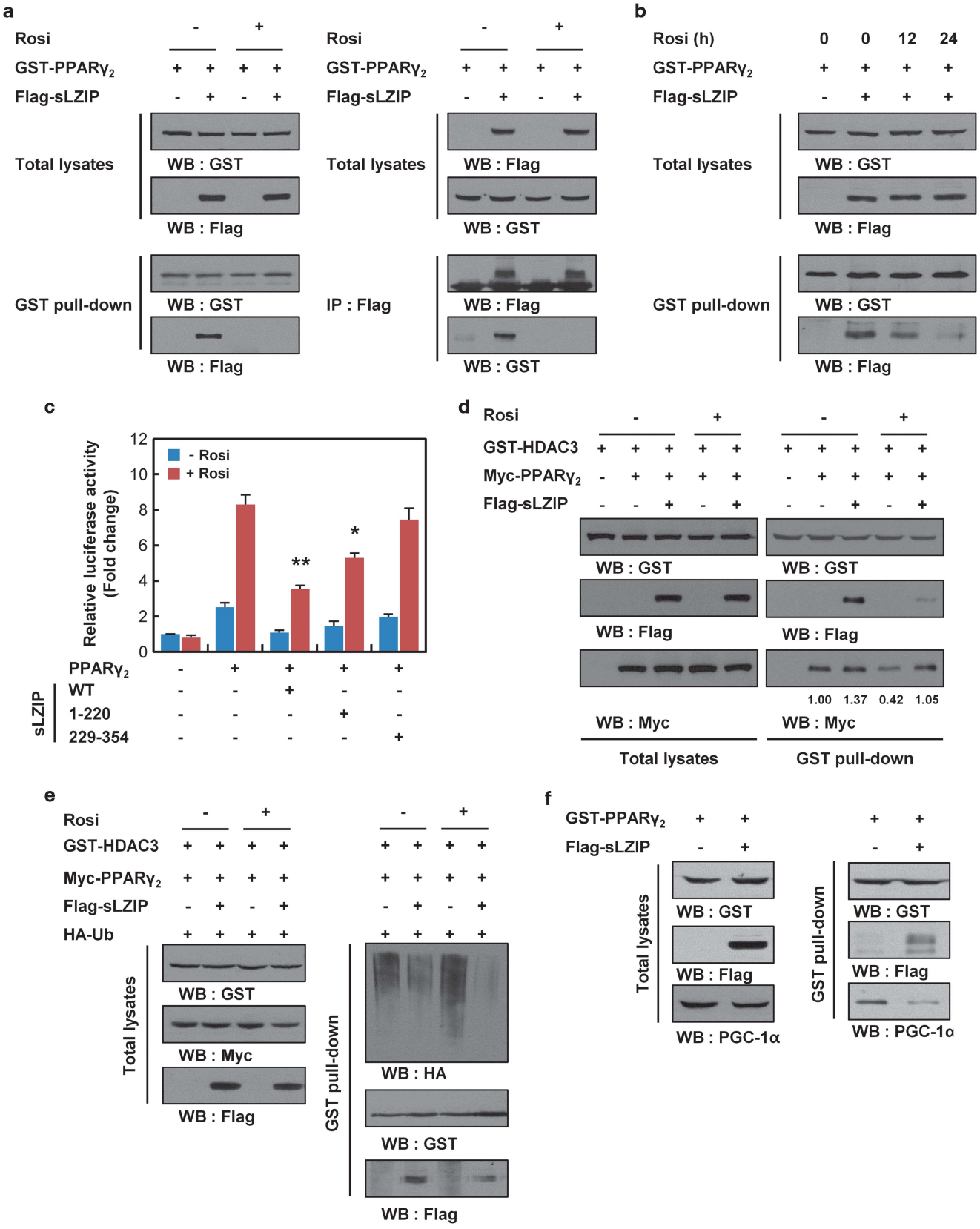
a
Rosi
GST-PPARγ2
Flag-sLZIP
Total lysates
WB : GST
WB : Flag
GST pull-down
IP : Flag
b
Rosi (h)
0 0 12 24
c
Relative luciferase activity (Fold change)
- Rosi
+ Rosi
PPARγ2
sLZIP
WT
1-220
229-354
d
GST-HDAC3
Myc-PPARγ2
WB : Myc
1.00 1.37 0.42 1.05
Total lysates
GST pull-down
e
HA-Ub
WB : HA
f
PGC-1α

embryos, from which heads and organs were removed.[27] Embryos were minced and digested using trypsin, and embryonic cells were grown in DMEM supplemented with 10% FBS and penicillin (100 U/ml)/streptomycin (100 μg/ml). Pre-adipocytes were isolated as previously described.[28] Briefly, primary pre-adipocytes were isolated from epididymal fat pads of WT and sLZIP TG mice using collagenase digestion and maintained in DMEM supplemented with 10% bovine calf serum and penicillin (100 U/ml)/streptomycin (100 μg/ml). ATDC5 cells were cultured in the medium consisting of a 1 : 1 mixture of DMEM and Ham's F-12 medium (Invitrogen) containing 5% FBS, 10 μg/ml human transferrin (Sigma-Aldrich), and 3×10^{-8} M sodium selenite (Sigma-Aldrich) and antibiotics. C3H10T1/2 and 293T cells were grown in DMEM containing 10% FBS and antibiotics. 3T3-L1 cells were grown in DMEM containing 10% bovine calf serum and antibiotics. Cells were cultured at 37 °C in a humidified incubator containing 5% CO_2. To induce adipocyte differentiation, primary human MSCs, primary pre-adipocytes, MEFs, C3H10T1/2, and 3T3-L1 cells were grown to confluence, and the media were replaced by DMEM containing 10% FBS, 5 μg/ml insulin, 1 μM dexamethasone, and 0.5 mM IBMX. To induce osteoblast differentiation, the media of MEFs and C3H10T1/2 cells were changed with DMEM containing 50 μg/ml ascorbic acid and 10 mM β-glycerophosphate. The differentiation media were replaced every 2 days. For induction of chondrogenesis, ATDC5 cells were treated with 10 μg/ml insulin in the medium.

Transient transfection and virus infection. Cells were plated in 60-mm culture dishes. After incubation for 24 h, cells were transfected using Lipofectamine 2000 (Invitrogen) or Genefectine (Genetrone Biotech., Qwangmyeong, South Korea) according to the manufacture's protocol. siRNAs were generated using sLZIP and HDAC target sequences in Supplementary Table S1. For RNA interference experiments, cells were transfected with scrambled siRNA and appropriate siRNAs using Lipofectamine 2000 reagent according to the manufacturer's instructions. Human MSCs were infected with an empty lentivirus or lentivirus-expressing human sLZIP shRNA. 3T3-L1 and C3H10T1/2 cells were infected with adenoviral vectors containing cDNA for human sLZIP or the empty vector at 50 MOI (multiplicity of infection). After 2 h, the infection medium was replaced by the fresh medium.

Semi-quantitative RT-PCR and quantitative real-time PCR. Total RNA was extracted using a TRIzol reagent (Invitrogen) according to the manufacturer's instructions. The first-strand cDNA was synthesized from 2 μg RNA using the Accupower RT PreMix (BioNeer, Daejeon, South Korea). Polymerase chain reaction (PCR) amplification was performed using the Hipi PCR Mix Kit (ELPIS-Biotech. Inc, Daejeon, South Korea) and the oligomers listed in Supplementary Table S2. GAPDH was amplified as an internal control. Real-time PCR was performed using LightCycler 480 with use of SYBR green master mix (Roche, Mannheim, Germany) and the oligomers listed in Supplementary Table S3. The ratio of target gene expression level over β-actin or GAPDH was calculated using a ΔCT method where the CT value is defined as the number of PCR cycle at which the fluorescent signal reaches a fixed threshold ratio of target. Each experiment was performed in three experimental replicates with three technical replicates within each experiment.

Luciferase reporter gene activity assay. Luciferase assays were performed using the Luciferase Assay System (Promega Corporation, Madison, WI, USA). Transfected cells were washed twice with ice-cold PBS and lysed in culture dishes using a reporter lysis buffer. Luciferase activities were recorded using a Luminometer 20/20^n (Turner BioSystems, Sunnyvale, CA, USA) according to the manufacturer's instructions. Luciferase activities were normalized to the β-galactosidase activity. For the β-galactosidase assay, pSV-β-galactosidase was co-transfected with the luciferase reporter gene. Cell extracts were assayed for the β-galactosidase activity using the β-galactosidase enzyme assay system (Promega) and analyzed using an ELISA plate reader (Bio-Rad Inc., Hercules, CA, USA). The ratio of the luciferase activity to the β-galactosidase activity was determined in triplicate samples. All data are presented as a mean ± S.D. of at least three independent experiments.

Electrophoretic mobility shift assay. Complementary oligonucleotides were annealed and labeled with [γ-^{32}P] ATP (Perkin Elmer, Waltham, MA, USA) using T4 polynucleotide kinase (Promega). Unincorporated nucleotide was removed by passage over a Bio-Gel P-6 spin column (Bio-Rad Inc.) as described by manufacturer's instructions. The His-sLZIP proteins were pre-incubated in the binding buffer (10 × GRAB, 20 mM DTT, Poly (dI-dC)) and incubated with radiolabeled probe for 20 min at room temperature. Each reaction mixture was then loaded on the well of a 6% non-denaturing polyacrylamide gel and electrophoresed in TBE buffer. For competition experiments, binding reactions were incubated with a 100-fold molar excess of unlabeled CREB-binding oligonucleotide for 30 min before addition of radiolabeled oligonucleotide. For supershift assay, anti-His antibody (Santa Cruz Biotechnology) was added to the reaction mixture for an additional 30 min on ice. The probes used for EMSA are listed in Supplementary Table S4.

ChIP. C3H10T1/2 cells grown in 100-mm culture dishes were infected with adenoviral HA-sLZIP. Following infection, cells were maintained in growth medium up to full confluence and medium was changed with differentiation medium. Cells were washed with 1 × PBS and treated with 1% formaldehyde in medium at room temperature for 10 min, followed by addition of glycine to a final concentration of 0.125 M for 5 min. Cells were scraped into PBS and centrifuged at 1000 × *g* for 5 min at 4 °C. ChIP assays were performed by co-precipitating the DNA-protein complexes with anti-HA antibody and anti-rabbit IgG as an internal control. The enhancer region of FABP4, which contains a functional CRE, was amplified from the prepared DNA using a primer pair: forward 5′-TAGCTGGAGAATCGCACAGA-3′ and reverse 5′-ACTTCCACTAGTGAACTCTGAT-3′.

Fluorescence microscopic analysis. Cells were grown on glass coverslips, washed twice with PBS, fixed in 4% paraformaldehyde for 10 min, and permeabilized with 0.2% Triton-X 100 for 5 min. Cells were incubated with 1% BSA for 1 h and with appropriate antibodies at 4 °C overnight. After washing with PBS, cells were incubated with Texas Red-conjugated antibodies for 2 h in the dark. Cover slides were washed with PBS, mounted, and examined using a LSM 700 META confocal microscope (Carl Zeiss, Jena, Germany).

sLZIP TG mice generation and bone histomorphometric analysis. For generation of human sLZIP TG mice, the sLZIP gene was cloned into the pCMV-Flag expression vector. sLZIP TG mice were generated by Macrogen Inc. (Seoul, South Korea). TG founders were mated with WT C57BL/6 mice to produce F1 heterozygotes. F1–F4 generations were genetically screened for the transgene at 2-week-old age. Following primers were used for amplification of the genomic DNA to identify WT and sLZIP TG mice: 5′-GGA CGA TGA TGA

Figure 4 sLZIP enhances formation of the PPARγ_2 corepressor complex. (**a**) 293T cells were transfected with GST-PPARγ_2 and Flag-sLZIP, and treated with or without 10 μM Rosi for 24 h. Cell lysates were collected and subjected to a GST pull-down assay using glutathione 4B beads. Cell extracts were analyzed by an immunoprecipitation assay using an anti-Flag antibody. (**b**) 293T cells were transfected with GST-PPARγ_2 and Flag-sLZIP, and treated with 10 μM Rosi for the indicated time periods. Cell lysates were subjected to a GST pull-down assay. (**c**) 293T cells were transfected with FABP4-Luc, β-galactosidase, PPARγ_2, and various sLZIP deletion mutants. Following transfection, cells were stimulated with or without 10 μM of Rosi for 24 h. Luciferase activities were normalized to the β-galactosidase activity and presented as the relative activity. All experiments were performed in triplicate and the bar represents the mean ± S.D. *$P<0.01$; **$P<0.005$. (**d**) 293T cells were transfected with GST-HDAC3, Myc-PPARγ_2, and Flag-sLZIP, then treated with or without 10 μM Rosi for 18 h. Cell lysates were subjected to a GST pull-down assay using glutathione 4B beads. (**e**) GST-HDAC3, Myc-PPARγ_2, Flag-sLZIP, and HA-Ub were expressed into 293T cells. Cells were then treated with 10 μM Rosi for 18 h. Cell lysates were subjected to a GST pull-down assay. (**f**) 293T cells were transfected with GST-PPARγ_2 and Flag-sLZIP, and treated with 10 μM Rosi for 24 h. Cell lysates were subjected to a GST pull-down assay. Protein complex was analyzed on SDS-PAGE followed by western blotting using anti-PGC1α, anti-GST, and anti-Flag antibodies

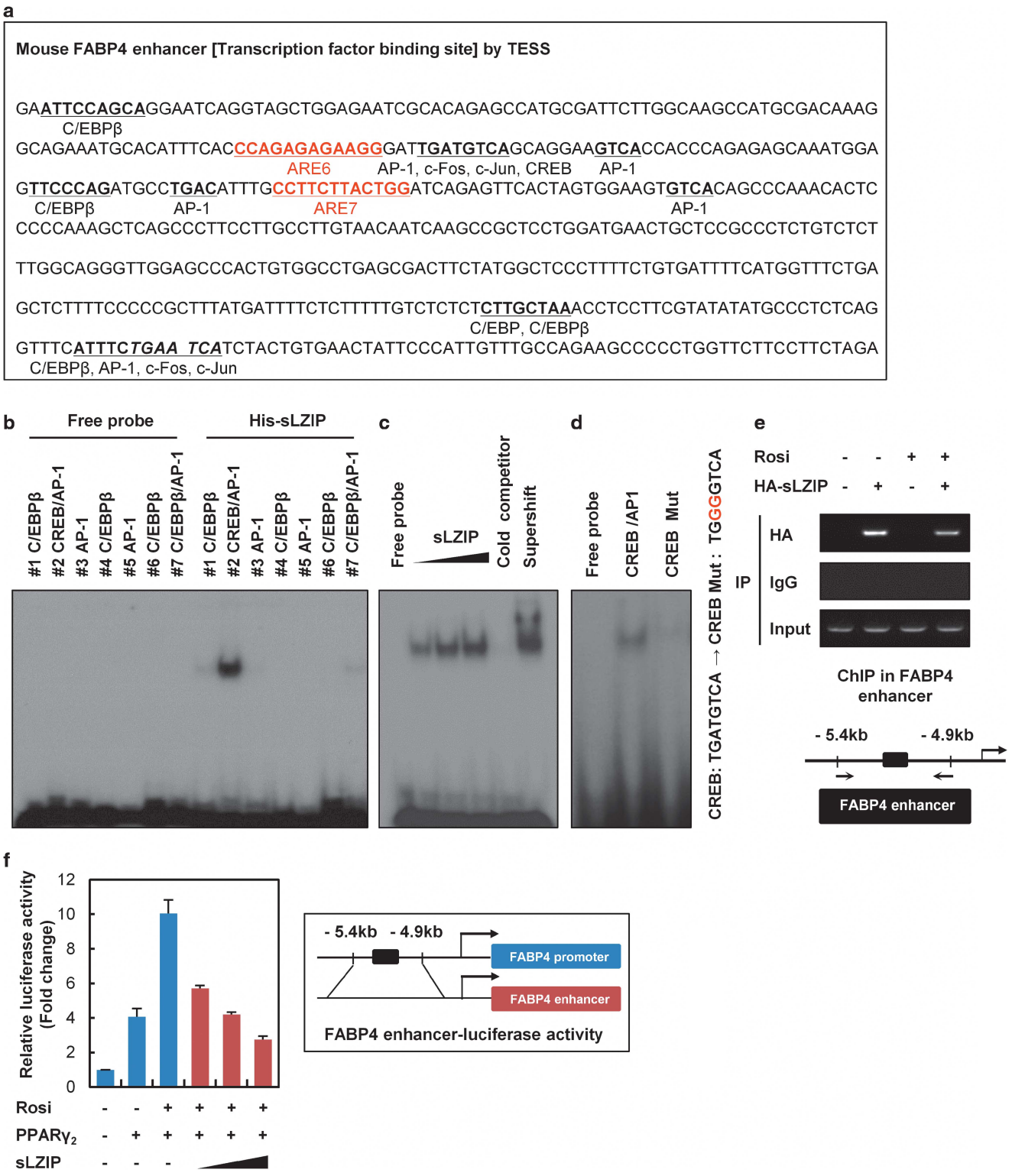

Figure 5 sLZIP binds to the enhancer region of FABP4. (**a**) Analysis of the FABP4 enhancer sequence by Transcription Element Search System and AliBaba2. (**b**) Recombinant His-sLZIP fusion protein (3 μg) was incubated with γ-^{32}P-labeled oligonucleotide probes containing the putative CREB-binding element. (**c**) γ-^{32}P-labeled oligonucleotide probes were incubated with increasing amounts of purified His-sLZIP. A competition assay was performed using a 100-fold molar excess of unlabeled CRE oligonucleotide probes. His antibody was added to the reaction mixture for a supershift assay. (**d**) His-sLZIP protein was subjected to an EMSA using WT and CRE mutants (TGATGTCA→TGGGGTCA). (**e**) C3H10T1/2 cells were infected with adenoviral HA-sLZIP and differentiated into adipocytes. After 8 days from post-induction, ChIP assays were performed using an antibody specific for HA-sLZIP. Input or immunoprecipitated chromatin was subjected to a PCR as a control for variations. (**f**) 293T cells were transfected with FABP4 enhancer-Luc, β-galactosidase, PPARγ_2, and various amounts of sLZIP (0.1, 0.25, and 0.5 μg). Following transfection, cells were stimulated with 10 μM Rosi for 24 h. Luciferase activities were normalized to the β-galactosidase activity and presented as the relative activity. All experiments were performed in triplicate and the bar represents the mean ± S.D.

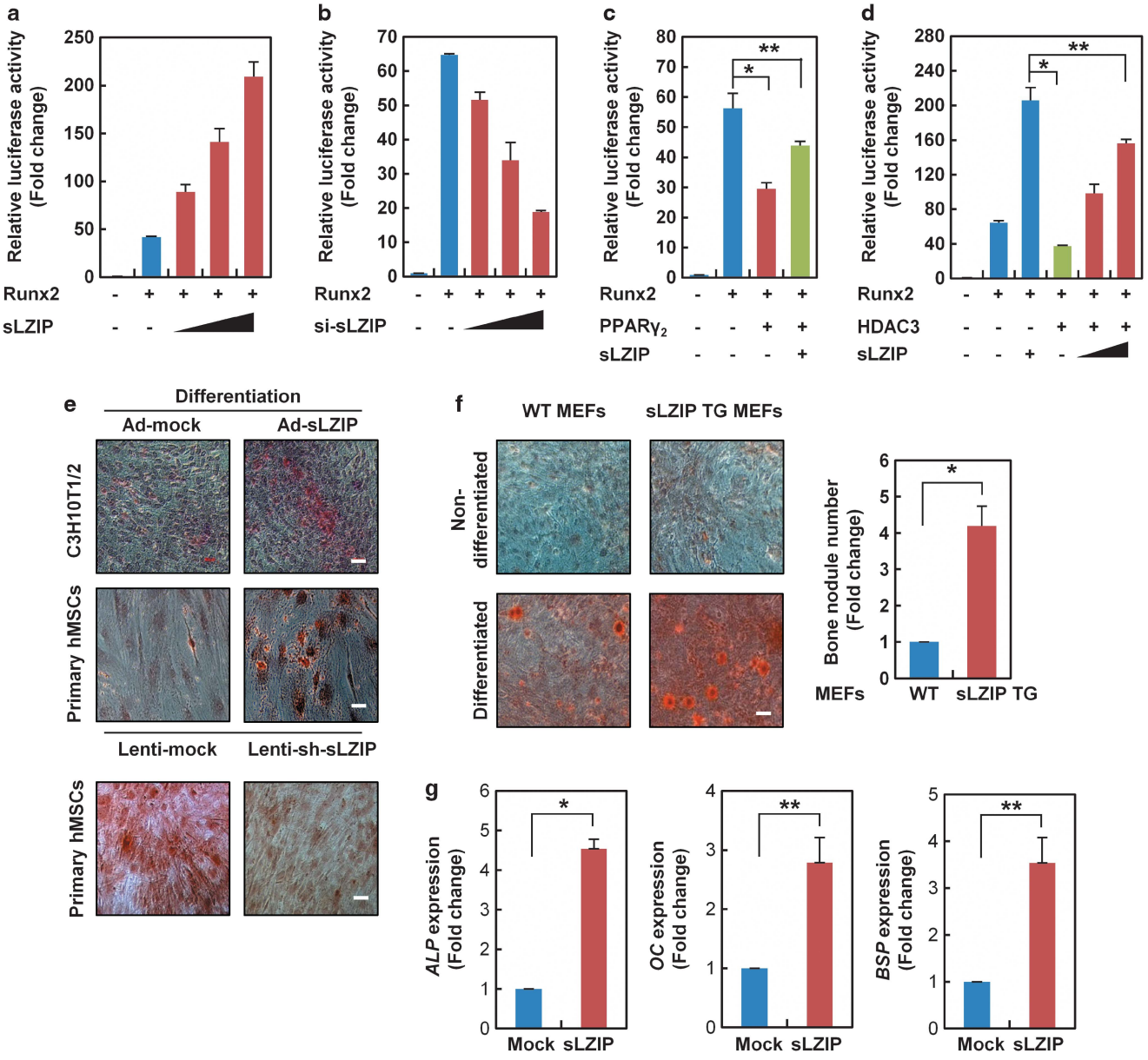

Figure 6 sLZIP promotes osteogenesis via enhancement of Runx2 transcriptional activity. (**a**) 293T cells were transfected with six copies of the Runx2 response element (OSE-Luc), β-galactosidase, Runx2, and various amounts of sLZIP (0.1, 0.25, and 0.5 μg). (**b**) 293T cells were transfected with OSE-Luc, β-galactosidase, Runx2, and various amounts of si-sLZIP (10, 50, and 100 nM). (**c**) 293T cells were transfected with OSE-Luc, β-galactosidase, PPARγ_2, Runx2, and sLZIP. (**d**) 293T cells were transfected with OSE-Luc, β-galactosidase, Runx2, HDAC3, and various amounts of sLZIP (0.25 and 0.5 μg). Promoter activity was determined by a luciferase assay. Luciferase activities were normalized to the β-galactosidase activity and presented as the relative activity. *$P<0.01$; **$P<0.005$. (**e**) Primary human MSCs and C3H10T1/2 cells were infected with sLZIP-expressing adenovirus or sLZIP shRNA expressing lentivirus, and differentiated into osteoblasts for 8 days. Scale bar, 50 μm. (**f**) MEF cells isolated from WT and sLZIP TG mice were differentiated into osteoblasts for 14 days. Cells were stained with Alizarin Red solution, and the number of nodules was counted. The number of bone nodules was counted in four randomly selected fields for each well, and data represent the mean of three independent experiments ± S.E.M. *$P<0.01$. Scale bar, 50 μm. (**g**) C3H10T1/2 cells were infected with sLZIP-expressing adenovirus and differentiated into osteoblasts for 8 days. Total RNA was extracted and the mRNA expression level of osteoblast marker genes (*APL, OC,* and *BSP*) were determined using real-time PCR. GAPDH was used as an internal control. *$P<0.001$, **$P<0.005$. All experiments were performed in triplicate and the bar represents the mean ± S.D.

CAA GGA CT-3′ and 5′-GTC AGA GGA GTA CAT GCT GCT-3′. sLZIP TG mice at embryonic day 12.5 (E12.5; cartilage) and 17.5 (E17.5; bone) were prepared and stained with Alizarin Red and Alcian Blue. Briefly, dissected embryos were rinsed with PBS and fixed in 95% ethanol for 24 h. The embryos were then transferred to staining solution consisting of 0.03% Alcian Blue 8GX and 0.5% Alizarin Red. After 24 h, tissues were dissolved by adding 2% KOH for 6 h, and rinsed with 20% glycerol/0.25% KOH for 24 h. Samples were then treated with 50% glycerol and 0.25% KOH for further clearing and storage. Micro-CT analyses were performed using Sky-Scan 1172 (Skyscan, Kontich, Belgium) and CT analyzer (Skyscan).

Statistical analysis. Data were presented as the mean ± S.D. Statistical evaluation was carried out using a one-way ANOVA. Data were considered statistically significant when $P<0.05$. All statistical analysis was performed using a computer program Prism (Graphpad Software, La Jolla, CA, USA).

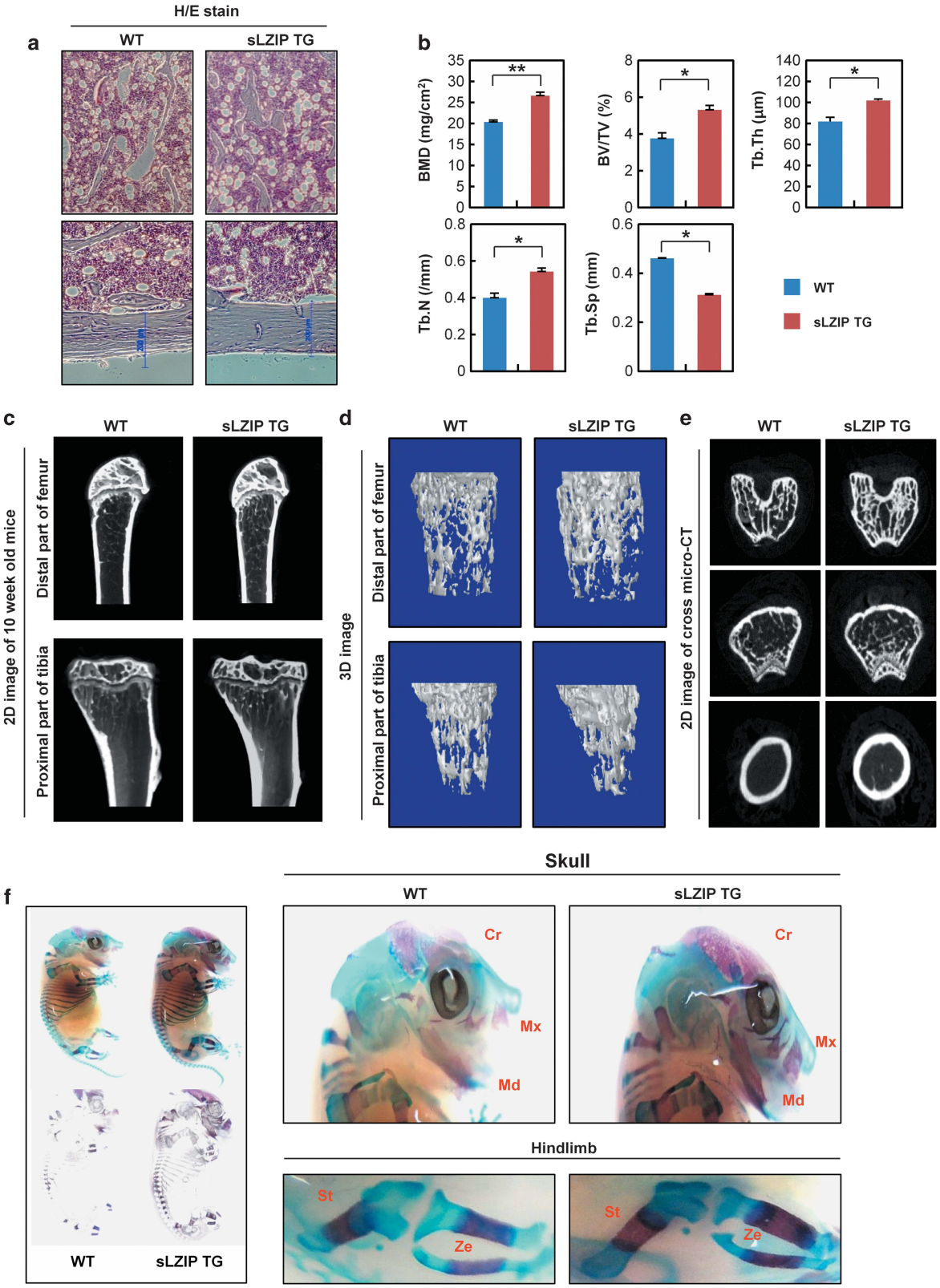

Figure 7 sLZIP enhances bone mass *in vivo*. (**a**) Hematoxylin/eosin staining of femurs in WT ($n=6$) and sLZIP TG ($n=5$) mice. (**b**) Histomorphometric analyses of bone mineral density (BMD), bone volume/tissue volume (BV/TV), trabecular thickness (Tb. Th.), bone number (Tb. N.), and separation (Tb. Sp.) in WT ($n=6$) and sLZIP TG ($n=5$) mice. $^{*}P<0.001$, $^{**}P<0.005$. (**c** and **d**) Micro-CT analysis of trabecular bones in femurs of 10-week-old WT ($n=6$) and sLZIP TG ($n=5$) mice. Two-dimensional (**c**) and three-dimensional (**d**) micro-CT analyses of distal part of femur and proximal part of tibia. (**e**) Cross-sectional images of the cortical bone. (**f**) Alizarin Red and Alcian Blue staining of mouse embryos at E17.5 stage ($n=5$) (Cr: cranium, Mx: maxilla, Md: mandible, St: stylopod, Ze: zeugopod)

Conflict of Interest

The authors declare no conflict of interest.

Acknowledgements. This research was supported by Basic Science Research Program through the National Research Foundation of Korea funded by the Ministry of Science, ICT and future Planning (2014R1A2A2A01002826).

1. Uccelli A, Moretta L, Pistoia V. Mesenchymal stem cells in health and disease. *Nat Rev Immunol* 2008; **8**: 726–736.
2. Kawai M, Rosen CJ. PPARgamma: a circadian transcription factor in adipogenesis and osteogenesis. *Nat Rev Endocrinol* 2010; **6**: 629–636.
3. Jeon MJ, Kim JA, Kwon SH, Kim SW, Park KS, Park SW *et al.* Activation of peroxisome proliferator-activated receptor-gamma inhibits the Runx2-mediated transcription of osteocalcin in osteoblasts. *J Biol Chem* 2003; **278**: 23270–23277.
4. Chandra V, Huang P, Hamuro Y, Raghuram S, Wang Y, Burris TP *et al.* Structure of the intact PPAR-gamma-RXR- nuclear receptor complex on DNA. *Nature* 2008; **456**: 350–356.
5. Tontonoz P, Hu E, Graves RA, Budavari AI, Spiegelman BM. mPPAR gamma 2: tissue-specific regulator of an adipocyte enhancer. *Genes Dev* 1994; **8**: 1224–1234.
6. Lehrke M, Lazar MA. The many faces of PPARgamma. *Cell* 2005; **123**: 993–999.
7. Perissi V, Aggarwal A, Glass CK, Rose DW, Rosenfeld MG. A corepressor/coactivator exchange complex required for transcriptional activation by nuclear receptors and other regulated transcription factors. *Cell* 2004; **116**: 511–526.
8. Yu C, Markan K, Temple KA, Deplewski D, Brady MJ, Cohen RN. The nuclear receptor corepressors NCoR and SMRT decrease peroxisome proliferator-activated receptor gamma transcriptional activity and repress 3T3-L1 adipogenesis. *J Biol Chem* 2005; **280**: 13600–13605.
9. Rosen ED, Hsu CH, Wang X, Sakai S, Freeman MW, Gonzalez FJ *et al.* C/EBPalpha induces adipogenesis through PPARgamma: a unified pathway. *Genes Dev* 2002; **16**: 22–26.
10. Fajas L, Egler V, Reiter R, Hansen J, Kristiansen K, Debril MB *et al.* The retinoblastoma-histone deacetylase 3 complex inhibits PPARgamma and adipocyte differentiation. *Dev Cell* 2002; **3**: 903–910.
11. Herzig S, Hedrick S, Morantte I, Koo SH, Galimi F, Montminy M. CREB controls hepatic lipid metabolism through nuclear hormone receptor PPAR-gamma. *Nature* 2003; **426**: 190–193.
12. Hong JH, Hwang ES, McManus MT, Amsterdam A, Tian Y, Kalmukova R *et al.* TAZ, a transcriptional modulator of mesenchymal stem cell differentiation. *Science* 2005; **309**: 1074–1078.
13. Chan CP, Kok KH, Jin DY. CREB3 subfamily transcription factors are not created equal: Recent insights from global analyses and animal models. *Cell Biosci* 2011; **1**: 6.
14. Luciano RL, Wilson AC. N-terminal transcriptional activation domain of LZIP comprises two LxxLL motifs and the host cell factor-1 binding motif. *Proc Natl Acad SciUSA* 2000; **97**: 10757–10762.
15. Kang H, Kim YS, Ko J. A novel isoform of human LZIP negatively regulates the transactivation of the glucocorticoid receptor. *Mol Endocrinol* 2009; **23**: 1746–1757.
16. Guan HP, Ishizuka T, Chui PC, Lehrke M, Lazar MA. Corepressors selectively control the transcriptional activity of PPARgamma in adipocytes. *Genes Dev* 2005; **19**: 453–461.
17. Sinha KM, Zhou X. Genetic and molecular control of Osterix in skeletal formation. *J Cell Biochem* 2013; **114**: 975–984.
18. Katagiri T, Takahashi N. Regulatory mechanisms of osteoblast and osteoclast differentiation. *Oral Dis* 2002; **8**: 147–159.
19. Rauch A, Seitz S, Baschant U, Schilling AF, Illing A, Stride B *et al.* Glucocorticoids suppress bone formation by attenuating osteoblast differentiation via the monomeric glucocorticoid receptor. *Cell Metab* 2010; **11**: 517–531.
20. Savkur RS, Burris TP. The coactivator LXXLL nuclear receptor recognition motif. *J Pept Res* 2004; **63**: 207–212.
21. Burbelo PD, Gabriel GC, Kibbey MC, Yamada Y, Kleinman HK, Weeks BS. LZIP-1 and LZIP-2: two novel members of the bZIP family. *Gene* 1994; **139**: 241–245.
22. Liu Y, Berendsen AD, Jia S, Lotinun S, Baron R, Ferrara N *et al.* Intracellular VEGF regulates the balance between osteoblast and adipocyte differentiation. *JClin Invest* 2012; **122**: 3101–3113.
23. Ichida F, Nishimura R, Hata K, Matsubara T, Ikeda F, Hisada K *et al.* Reciprocal roles of MSX2 in regulation of osteoblast and adipocyte differentiation. *J Biol Chem* 2004; **279**: 34015–34022.
24. Wang YX. PPARs: diverse regulators in energy metabolism and metabolic diseases. *Cell Res* 2010; **20**: 124–137.
25. Schwartz AV, Sellmeyer DE, Vittinghoff E, Palermo L, Lecka-Czernik B, Feingold KR *et al.* Thiazolidinedione use and bone loss in older diabetic adults. *JClin Endocrinol Metab* 2006; **91**: 3349–3354.
26. Murakami T, Saito A, Hino S, Kondo S, Kanemoto S, Chihara K *et al.* Signalling mediated by the endoplasmic reticulum stress transducer OASIS is involved in bone formation. *Nat Cell Biol* 2009; **11**: 1205–1211.
27. Zhang JW, Klemm DJ, Vinson C, Lane MD. Role of CREB in transcriptional regulation of CCAAT/enhancer-binding protein beta gene during adipogenesis. *J Biol Chem* 2004; **279**: 4471–4478.
28. Shillabeer G, Lau DC. Regulation of new fat cell formation in rats: the role of dietary fats. *J Lipid Res* 1994; **35**: 592–600.

Supplementary Information accompanies this paper on Cell Death and Differentiation website (http://www.nature.com/cdd)